Supplementary Information

Ni Substitutional Defects in Bulk and at the (001) Surface of MgO from First-Principles Calculations

Aliaksei Mazheika* and Sergey V. Levchenko

Fritz-Haber-Institut der Max-Planck-Gesellschaft, Faradayweg 4-6, 14195 Berlin, Germany

Computational details

CCSD(T) calculations of CO, CO_2, and H_2 adsorption energies at Ni_{Mg} defects at the MgO(001) surface, as well as formation energies of bulk Ni_{Mg}, are performed using ORCA electronic-structure package, which is based on Gaussian-type orbitals [1]. For bulk Ni_{Mg} defects, $NiMg_{12}O_6(PP)_{50}$ cluster is used (Fig. 1c in main text), where PP denotes electron-free Hay-Wadt effective-core potentials (ECPs) [2] replacing Mg^{2+} cations. The cluster is immersed in an array of point charges (145 $+2|e|$ charges replacing Mg^{2+} and 194 $-2|e|$ charges replacing O^{2-}). 14 electrons are removed to ensure bulk-like ionization states of all the atoms. The positions of the atoms, ECPs, and point charges in the bulk cluster models are generated by cutting out a cube centered on a Mg atom from the bulk MgO structure with 4.211 Å) lattice constant, with no further relaxation. The lattice constant was obtained from standard HSE06 calculations (see below for details). For surface Ni_{Mg} defects, two models were used: terrace-site and monolayer-step (Fig. 1a-b in main text), both have the stoichiometry $NiMg_8O_9(PP)_{49}$. The structure of the terrace-site cluster was generated as follows. First, a periodic slab model of MgO (001) (2x2 surface unit cell and 4 atomic layers) with a Ni_{Mg} defect and possibly an adsorbed molecule is relaxed at HSE06 level with *tight* basis set and 4x4x4 k-points. Second, the cluster around the Ni_{Mg} defect was cut out of the slab and immersed into an array of point charges and pseudopotentials. The geometry of embedding corresponded to ideal bulk-like structure. Since the relaxation of (sub)surface atomic layers is pronounced very slightly even with Ni, such embedding geometry matches cluster structure well. In the case of monolayer-step cluster, similar strategy was applied. The 4-atomic layer MgO(001) slab (2x3 surface unit cell) with a periodically translated along *x*-axe (2x2) "monolayer-island" and with/without adsorbate molecule was fully relaxed at HSE06 level. The cluster with Ni_{Mg} defect was cut from it and embedded like in the other cases. For all cluster models, the target properties were converged with respect to the number of shells of pseudopotentials and point charges at PBE level. Collinear spin-unrestricted calculations are performed, unless otherwise specified, with spin-moment projection fixed to $S_z = 1$, which is found to be the ground spin-state of the neutral Ni_{Mg} defect for all α. The spin-states of charged defects are discussed in the main text.

In the CCSD(T) calculations, cc-pV*X*Z [3] basis sets are employed, with X = D for Mg and O, and X = T for all atoms in adsorbed species and surface atom underneath (Ni or O). For adsorption and defect formation energies, counterpoise basis-set superposition error (BSSE) correction is applied. The excitations from 1s-3p orbitals of Ni, 1s-2p of Mg, 1s of O and C were excluded from the coupled-cluster calculations (frozen-core approximation). These settings were the best we could afford with our embedded cluster models. However, we estimate the complete basis-set (CBS) limit for CCSD(T) by combining the extrapolation of MP2 energies to CBS limit with the so-called “focal-point” method [4] which is based on the observation that the difference in correlation energies obtained in different methods converges with the basis set size much faster than the total energies. For the extrapolation of MP2 energies to CBS limit different methods were tested: the 2 points method which was proposed in

the original article [5] and least squares regression in which all points were considered and extrapolated with an exponential function. The difference in observed values for all approaches usually did not exceed 38 meV.

For DFT and G_0W_0 calculations, we use the all-electron numeric atomic-orbital based electronic-structure package FHI-aims [6]. The same cluster models are used as described above, but with norm-conserving non-local pseudopotentials [7] replacing Mg^{2+} ECPs. Standard *tight* numerical settings are employed. The extrapolation to CBS limit is performed using valence-consistent numeric atomic orbitals (NAO-VCC-*X*Z, with *X* = D, T, Q, 5) [5]. HSE06 exchange-correlation functional with variable α [further denoted HSE(α)], as implemented in FHI-aims [8], is used. The reference for G_0W_0 [9] calculations is HSE(α). In our study the value of the HSE screening parameter ω [10] was fixed to the standard value 0.11 $bohr^{-1}$ [11]. Another ω value 0.0 $bohr^{-1}$ with α = 0.25 (PBE0) was also tested, but was found to have a small effect on target properties. The fraction of exact exchange α is varied between 0 (corresponds to PBE) and 1.

In addition to the cluster model $NiMg_{12}O_6(PP)_{50}(+2)_{6028}(-2)_{6078}$, a larger cluster model $NiMg_{18}O_{14}(PP)_{44}(+2)_{7610}(-2)_{7654}$ (Fig. 1d in main text) was considered for G_0W_0 calculations. Also for surface, to test cluster-size dependence, larger models $NiMg_{13}O_9PP_{81}(+2)_{3084}(-2)_{3165}$, $NiMg_{12}O_{13}PP_{45}(+2)_{775}(-2)_{820}$ and $NiMg_{29}O_{30}PP_{97}(+2)_{3936}(-2)_{4033}$ were employed.

The dependence of the adsorption energies on cluster size was also tested for CO and CO_2 adsorption. The HSE(0.3) CO adsorption energy was found to be higher (in absolute value) at the $NiMg_{13}O_9$ embedded cluster compared to the smaller cluster $NiMg_8O_9$ (-0.60 eV and -0.46 eV, respectively). The MP2 adsorption energy of CO at the larger cluster is -0.56 eV versus -0.40 eV at the smaller one. However, the difference E_{ads}(MP2) - E_{ads}(HSE(0.3)) = 0.04 eV is still the same as in the case of the smaller embedded cluster $NiMg_8O_9$ for which CCSD(T) calculations were done. The energy of CO binding to the largest $NiMg_{29}O_{30}$ embedded cluster calculated with HSE(0.3) is about -0.37 eV, which is already very close to the value obtained with the periodic slab model (see main text). In the case of CO_2-adsorption, the HSE(0.3) energy on $NiMg_{12}O_{13}$ embedded cluster was found to be lower in absolute value than on $NiMg_8O_9$ embedded-cluster, -2.90 eV vs. -3.50 eV. However, as in the case of CO, the MP2 adsorption energy is also lower, and the difference E_{ads}(MP2) - E_{ads}(HSE(0.3)) = 0.14 eV for bigger cluster is almost the same as for the smaller one (0.16 eV). This shows that the optimal α does not depend on the cluster size, and that α = 0.3 is a good compromise for calculating adsorption energies of different molecules at Ni-doped MgO surfaces.

In addition to MP2 calculations, exact-exchange plus correlation in random-phase approximation (RPA), renormalized single excitation (rSE) contributions, and second-order screened exchange (SOSEX) contributions were calculated with FHI-aims [12] for benchmarking purposes. The reference state in all RPA-based methods is obtained with PBE.

In periodic HSE(α) calculations, the number of k-points was set for each particular supercell (bulk: 2x2x2, 3x3x3, 4x4x4; slabs: 2x2, 2x3, 3x3, 4x4) by scaling down the 8x8x8 Γ-centered grid used for the cubic 8-atom MgO unit cell. The underlying lattice parameter was set to 4.211 Å, as obtained with HSE06 functional and as it was done in the validation part. The MgO(001) surface is modelled by a 5-atomic-layer slab in which all atoms are allowed to relax. The vacuum gap is set to about 250 Å. Nevertheless, the dipole correction was included and was found to be negligible. The numeric parameters and basis sets correspond to standard *tight* settings. Geometry optimization was done using BFGS algorithm with the accuracy of forces 10^{-4} eV/Å, until the maximum component of force on any atom did not exceed 10^{-2} eV/Å.

Many-body-dispersion (MBD) calculations were done with advanced dispersion coefficients for Mg and O substrate ions [13].

Influence of random-phase approximation (RPA) and beyond RPA on adsorption

RPA underestimates adsorption energy by 0.14-0.22 eV compared to CCSD(T), that is not unexpected [12]. The effect of inclusion of rSE and SOSEX depends on the adsorbed molecule: RPA+rSE significantly overestimates the CO adsorption energy (by 0.48 eV), while inclusion of SOSEX remedies to some extend the obvious failure of rSE but the adsorption energy is still overestimated by 0.24 eV. In the case of CO_2 on Ni_{Mg}MgO-step, rSE almost does not affect the adsorption, whereas SOSEX leads to overestimation of adsorption energy by almost the same value, 0.27 eV. The failure of the RPA-based methods could be due to the absence of ladder-type diagrams, which describe the short-range correlation [12] and which are present in CCSD(T). The short-range correlation is expected to be important for Ni ion containing 8 *d*-electrons in one shell. In order to confirm this, we have calculated CO@MgO adsorption energy using the same cluster model (exactly same geometry including the adsorbed molecule) but with Mg replacing Ni. The results are also presented in Table 1 in main text. Note that the CCSD(T) adsorption energy is positive in this case. It was found in previous studies that CO is physisorbed on pure MgO surface with electrostatic and dispersion forces [14,15]. We find that RPA still underestimates the adsorption energy by almost the same amount as in the case of CO@Ni_{Mg}MgO, -0.14 eV. RPA+rSE and rPT2 overestimate the adsorption energy, but the deviation is lower, 0.20 and 0.17 eV, respectively. Obviously, the short-range correlation of *d*-electrons plays an important role, but its absence is not the only reason for the failure of RPA. From Table 1 one can see that including SOSEX is important in the case of Ni defect, whereas for pure MgO it improves the adsorption energy by only 0.03 eV.

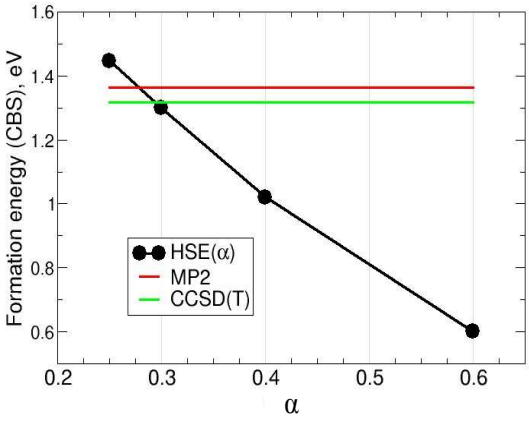

Figure S1. Formation energies of Ni_{Mg} at the (001) terrace obtained with different methods.

Validation of ionization potentials

The ionization energy can be in principle calculated as the difference between the total ground-state energies of the ionized and the neutral systems. However, a large spin-contamination in the Hartree-Fock reference, and the analysis of T_1 amplitudes in our coupled-cluster calculations, show that the Ni_{Mg} defect with one electron removed is a multireference system, namely, excitations from VBM to the e_{2g}-originating states generate electronic configurations that are quasi-degenerate with both the doublet and the quadruplet spin-states of $(Ni_{Mg})^+$. The G_0W_0@HSE(α) approach, on the other hand,

does not suffer from this problem, since the reference state (the neutral system) can be described by a single Slater determinant for any α.

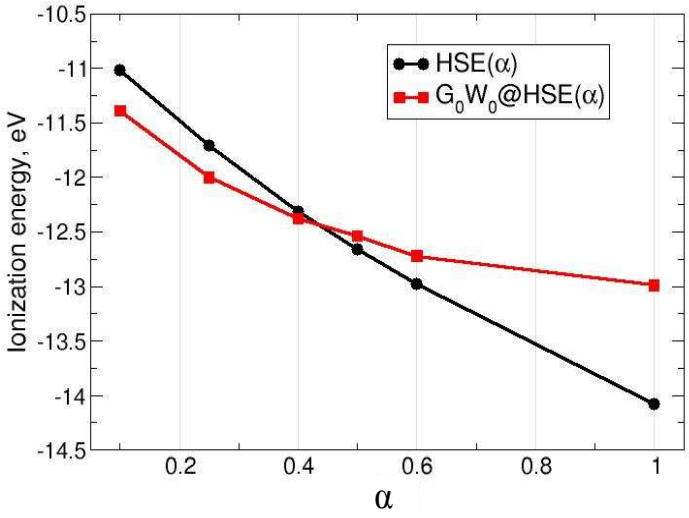

Fig. S2. Vertical ionization energies of $NiMg_{12}O_6$ embedded cluster calculated with different methods.

References.

1. Neese, F. **2012**.

2. Hay, P. J.; Wadt, W.R. *Ab initio* Effective Core Potentials for Molecular Calculations. Potentials for K to Au Including the Outermost Core Orbitals. *J. Chem. Phys.*, **1985**, *82*, 299.

3. Dunning, T.H., Jr. Gaussian Basis Sets for Use in Correlated Molecular Calculations. I. The Atoms Boron Through Neon and Hydrogen. *J. Chem. Phys.* **1989**, *90*, 1007-1023. Balabanov, N.B.; Peterson, K.A. Systematically Convergent Basis Sets for Transition Metals. I. All-Electron Correlation Consistent Basis Sets for the 3d Elements Sc-Zn. *J. Chem. Phys.*, **2005**, *123*, 064107.

4. Jurečka, P.; Šponer, J.; Černý, J.; Hobza, P. Benchmark Database of Accurate (MP2 and CCSD(T) Complete Basis Set Llimit) Interaction Energies of Small Model Complexes, DNA Base Pairs, and Pairs. *PCCP*. **2006**, *8*, 1985-1993. Řezáč, J.; Riley, K.E.; Hobza, P. S66: A Well-balanced Database of Benchmark Interaction Energies Relevant to Biomolecular Structures. *JCTC*, **2011**, *7*, 2427-2438.

5. Zhang, I.Y.; Ren, X.; Rinke, P.; Blum, V.; Scheffler, M. Numeric Atom-Centered-Orbital Basis Sets with Valence-Correlation Consistency from H to Ar. *New J. Phys.*, **2013**, *15*, 123033(1-31).

6. Blum, V.; Gehrke, R.; Hanke, F.; Havu, P.; Havu, V.; Ren, X.; Reuter, K.; Scheffler, M. Ab initio Molecular Simulations with Numeric Atom-Centered Orbitals. *Comput. Phys. Comm.*, **2009**, *180*, 2175-2196.

7. Fuchs, M.; Scheffler, M. Ab initio Pseudopotentials for Electronic Structure Calculations of Poly-Atomic Systems Using Density-Functional Theory. *Comp. Phys. Comm.*, **1998**, *119(1)*, 67-98.

8. Levchenko, S.V; Ren, X.; Wieferink, J.; Johanni, R.; Rinke, P.; Blum V.; Scheffler, M. Hybrid Functionals for Large Periodic Systems in an All-Electron, Numeric Atom-Centered Basis Framework. *Comp. Phys. Comm.*, **2015**, *192*, 60-69.

9. Ren, X.; Rinke, P.; Blum, V.; Wieferink, J.; Tkatchenko, A.; Sanfilippo, A.; Reuter, K.; Scheffler, M. Resolution-of-identity approach to Hartree-Fock, hybrid density functionals, RPA, MP2, and GW with numeric atom-centered orbital basis functions. *New J. Phys.*, **2012**, *14*, 053020.

10. Heyd, J.; Scuseria, G.E.; Ernzerhof, M. Hybrid Functionals Based on a Screened Coulomb Potential. *J. Chem. Phys.*, **2003**, *118*, 8207-8215.

11. Krukau, A.V.; Vydrov, O.A.; Izmaylov, A.F.; Scuseria, G.E. Influence of the Exchange Screening Parameter on the Performance of Screened Hybrid Functionals. *J. Chem. Phys*., **2006**, *125*, 224106(1-5).

12. Ren, X.; Rinke, P.; Joas, C.; Scheffler, M. Random-Phase Approximation and its Applications in Computational Chemistry and Materials Science. *J. Mater. Sci*., **2012**, *47*, 7447-7471.

13. Zhang, G.X.; Tkatchenko, A.; Paier, J.; Appel, H.; Scheffler, M. van der Waals Interactions in Ionic and Semiconductor Solids. *Phys. Rev. Lett*., **2011**, *107*, 245501.

14. Staemmler, V. Method of Local Increments for the Calculation of Adsorption Energies of Atoms and Small Molecules on Solid Surfaces. 2. CO/MgO(001). *J. Phys. Chem. A*, **2011**, *115*, 7153-7160.

15. Boese, A.D.; Sauer, J. Accurate Adsorption Energies of Small Molecules on Oxide Surfaces: CO–MgO(001) *PhysChemChemPhys*, **2013**, *15*, 16481-16493.